ANTIOXIDANTS & REDOX SIGNALING
Volume 9, Number 8, 2007

DOI: 10.1089/ars.2007.1594

Original Research Communication

Vascular Smooth Muscle NO Exposure from Intraerythrocytic SNOHb: A Mathematical Model

KEJING CHEN,[1] ROLAND N. PITTMAN,[2] and ALEKSANDER S. POPEL[1]

ABSTRACT

We previously constructed computational models based on the biochemical pathway analysis of different nitric oxide (NO) synthase isoforms and found a large discrepancy between our predictions and perivascular NO measurements, suggesting the existence of nonenzymatic sources of NO. *S*-nitrosohemoglobin (SNOHb) has been suggested as a major source to release NO in the arteriolar lumen and induce hypoxic vasodilation. In the present study, we formulated a multicellular computational model to quantify NO exposure in arteriolar smooth muscle when the NO released by intraerythrocytic SNOHb is the sole NO source in the vasculature. Our calculations show an NO exposure of ~0.25–6 p*M* in the smooth muscle region. This amount does not account for the large discrepancy we encountered regarding perivascular NO levels. We also found that the amount of NO delivered by SNOHb to smooth muscle strongly depends on the SNOHb concentration and half-life, which further determine the rate of NO release, as well as on the membrane permeability of red blood cells (RBCs) to NO. In conclusion, our mathematical model predicts that picomolar amounts of NO can be delivered to the vascular smooth muscle by intraerythrocytic SNOHb; this amount of NO alone appears not sufficient to induce the hypoxic vasodilation. *Antioxid. Redox Signal.* 9, 1097–1110.

INTRODUCTION

Nitric oxide (NO) is an uncharged free radical with diverse physiologic and pathologic functions. In the vascular system, NO is a potent vasodilator that regulates vascular tone by activating soluble guanylate cyclase (sGC), which further catalyzes the formation of 3′,5′-cyclic guanosine monophosphate (cGMP) (1). NO can also modify protein activities through *S*-nitrosylation (20). NO can be formed as a result of catalysis by nitric oxide synthase (NOS) through a five-electron transfer cycle. To date, three isoforms of NOS have been identified: neuronal NOS (nNOS or NOS1), inducible NOS (iNOS or NOS2), and endothelial NOS (eNOS or NOS3). NO could also be synthesized by mitochondrial nitric oxide synthase (mtNOS), but the existence of this enzyme is still under debate (11, 30). NOS3-derived NO has been regarded as the major source of the NO that induces vasodilation in the vasculature, including the microvasculature (16).

Perivascular NO concentrations have been measured by using microelectrodes, and the values reported are generally in the range of several hundred nanomolar (47, 51, 53); the measured NO has been attributed to the endothelial sources. However, although electrochemical methods for *in vivo* NO measurements have achieved significant success in quantifying the NO concentration in some tissues (44), our knowledge and understanding of NO production from specific sources remain limited. Immunohistochemical experiments and fluorescence measurements by using 4,5-diaminofluorescein diacetate have shown that nonendothelial sources of NO, both enzymatic and nonenzymatic, play significant roles in the regulation of vasodilation (18, 24). Furthermore, our biochemical pathway analyses (7) have shown that NOS3-derived NO cannot account for

[1]Department of Biomedical Engineering, Johns Hopkins University School of Medicine, Baltimore, Maryland.
[2]Department of Physiology, Medical College of Virginia Campus, Virginia Commonwealth University, Richmond, Virginia.

the large concentration of NO measured in the perivascular region. Our subsequent computational study of the NO concentration profile in the microvasculature, by using an NO release rate based on biochemical pathway analyses of multiple NOS isoforms (NOS1 and NOS3) (8), showed that a discrepancy between the predicted and measured values still exist, although NOS1-derived NO levels could be much higher than those of NOS3-derived NO because of the higher expression, faster catalysis, more distant location of NOS1 from the lumen where strong scavenging effects by hemoglobin occur.

It has been suggested that a significant portion of the fluorescence signal obtained during *in vivo* measurements came from intraluminal sources (43). The investigation of the fate of NO in the lumen, with its red blood cells (RBCs) containing a high concentration of hemoglobin (Hb), has a long history. Because of the rapid reactions occurring between NO and erythrocytic hemoglobin (both oxygenated and deoxygenated), blood in the vessel lumen has long been regarded as a potent NO scavenger (25, 31, 48). In the 1990s, Stamler and co-workers (23) proposed a novel endocrine signaling pathway involving the preservation of NO bioactivity by certain blood proteins (*e.g.*, hemoglobin). This view was later developed into the *S*-nitrosohemoglobin (SNOHb) hypothesis, in which NO binds to T state (deoxygenated) hemoglobin to form $Fe^{2+}NO$. The NO molecule is then transferred from the ferrous iron group to the cysteine residue at position 93 on the β chains (β-93 cysteine), where the NO bioactivity is preserved. Under hypoxic conditions, Hb undergoes allosteric changes that result in the transfer of NO to the thiols of the anion-exchange protein present on the membrane, or to glutathione by a transnitrosation. It is then further exported from the RBCs and induces vasodilation (2, 40). It is not yet clear whether the nitrogen oxides (NO_x) released from RBCs are in the form of nitrogen monoxide (free NO) (36, 52) or other NO equivalents (15). However, experimental observations have demonstrated significant nonenzymatic NO production within the vessel lumen (43).

Despite intensive investigation of erythrocytic SNOHb as a vasodilator, little quantitative knowledge exists of the transport and distribution of SNOHb-released NO. This quantitative question has presented a conceptual problem: whether SNOHb-delivered NO is sufficient to induce vascular smooth muscle relaxation through the known NO-sGC-cGMP pathway (13). In the present study, we used a mathematical model to analyze the NO released through the RBC pathway and predict the NO concentration in the vascular smooth muscle cells. We also compared the contribution of the intravascular NO source with that of vascular and perivascular enzymatic sources.

MODEL FORMULATION

Model geometry and assumptions

We have now formulated a reaction-diffusion model of NO transport in and around microvessels to predict the NO concentration in vascular smooth muscle when NO is released from the intraluminal SNOHb (Fig. 1). The NO released from RBCs is the only source of NO-induced vasodilation in our model. The cross section of an arteriole with its surrounding tissue is modeled, and a discrete distribution of RBCs is considered in the lumen. For the sake of simplicity, the model is two-dimensional (*i.e.*, a single vessel cross section is considered); the model can be readily extended to three dimensions. The model, as illustrated in Fig. 1, consists of five layers:

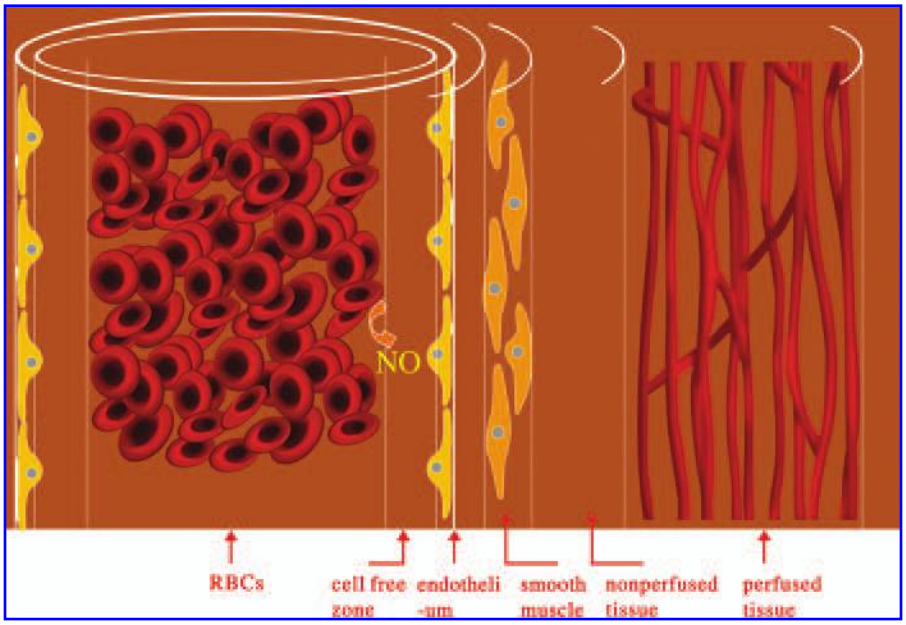

FIG. 1. Model schematic. Five layers exist in the model: (1) the intraluminal layer containing discrete RBCs and plasma, with NO being released from the SNOHb in erythrocytes; (2) endothelium and associated interstitial space; (3) smooth muscle cells containing sGC that catalyzes the formation of cGMP; (4) nonperfused tissue containing nerve fibers and parenchymal cells; and (5) tissue perfused by capillaries. NO released by the intraerythrocytic SNOHb is the sole source of NO in the model. (For interpretation of the references to color in this figure legend, the reader is referred to the web version of this article at www.liebertonline.com/ars)

Layer 1, the intraluminal layer containing discrete RBCs and plasma. In this layer, NO can be released from the intraerythrocytic SNOHb. RBCs are modeled as circles; other shapes can be used, but the geometry is not expected to affect the conclusions (22). Because the RBC membrane possesses an intrinsic resistance to NO diffusion (4, 10, 22), the RBC is further divided into two subregions: a thin membrane and the homogeneous intraerythrocytic hemoglobin.
Layer 2, endothelium and associated interstitial space.
Layer 3, smooth muscle cells containing sGC that catalyzes the formation of cGMP.
Layer 4, nonperfused tissue containing nerve fibers and parenchymal cells.
Layer 5, tissue perfused by capillaries.

Each of the five layers is represented as a circle, and the size (radius) of each layer, based on experimental data for arterioles, is listed in Table 1. The number of intraluminal RBCs corresponds to 45% hematocrit (39). It is recognized that the *in vivo* vessel hematocrit in arterioles may be significantly smaller than 45%, corresponding to systemic hematocrit (32). In our simulations, we considered a wide range of hematocrit values between 7 and 60%, and we showed that the NO concentration increases somewhat with higher hematocrit. When a 45% hematocrit value is used, the area occupied by the RBCs in the lumen accounts for 45% of the total luminal cross section. Calculations were performed for both a regular and a random distribution of RBCs, with the constraint that no overlap be present between RBCs; we will show that no significant difference occurred between the results of the calculations derived from different types of distributions. When a physiologic RBC-free layer was considered, RBC positioning was limited by the rule that no part of a RBC could be in the RBC-free region.

To make the model tractable yet retain the most important features, we made the following assumptions:

1. The effect of convection is insignificant because the Damkohler number ($D_a = \frac{k_b L}{U}$), which represents the ratio of reaction to convection, is estimated as 173 when the effective consumption rate of NO by blood (k_b) is 1,300 per second, the arteriole length (L) is 1,000 μm, and the velocity of blood flow (U) is 7,500 μm/s (27). Thus, we ignore the convection effect based on the large Damkohler number.
2. No enzymatic NO production is considered. The NOS-derived NO is ignored in calculations because of the focus on the RBC-released NO; enzymatic NO production has been investigated in our previous publications (7, 8).
3. The SNOHb concentration does not change with time. SNOHb can be consumed during hypoxic vasodilation, but it also can be replenished by blood flow, NO rebinding, and further synthesis using substrates such as nitrite (3). Moreover, we assume that the NO release from RBCs does not change over time, although SNOHb consumption and NO rebinding to Hb may affect the NO rate.
4. Although the exact fate of the nitrosonium released from the β-93 cysteine still remains to be elucidated (2, 15, 36), we assume the exported NO bioactivity from RBCs is in the form of nitrogen monoxide (free NO), which diffuses to the target smooth muscle.

Governing equations and chemical reactions

The governing equation describing the diffusion of NO and the reactions of NO with the reactive species present in the vascular region are as follows:

$$\frac{\partial C_{NO}}{\partial t} = D_{NO}\nabla^2 C_{NO} + R_{NO} \quad (1)$$

where C_{NO} is the NO concentration, D_{NO} is the diffusivity of NO, and R_{NO} is the sum of total production and consumption rates of NO. Here we considered the system at steady state $\left(\frac{\partial C_{NO}}{\partial t} = 0\right)$. The governing equation was applied to all regions described earlier.

Both sources and sinks of NO exist in the described regions. In the perfused tissue layer (layer 5), NO is consumed mainly by oxygen and hemoglobin contained in RBCs flowing through the capillaries. Also, we do not consider the NO production by the capillary endothelium, because we are focusing on the RBC-induced hypoxic vasodilation. Moreover, no intracapillary NO production by SNOHb is considered in this layer because the nonenzymatic NO release from RBCs is observed only in precapillary arterioles (40). In the nonperfused tissue layer (layer 4), no NO production exists, because the NOS activity is ignored when we focus on the NO vasodilation under hypoxic conditions. Also, NO is consumed in this layer through its reactions with oxygen. Here we also ignore the NO consumption by parenchymal tissue that occurs through an oxygen-dependent mechanism (45) because of the hypoxic conditions. In the smooth muscle layer (layer 3), NO is consumed through reactions with sGC, resulting in vasodilation. In the endothelium and the interstitial space (layer 2), NO is consumed through reactions with oxygen; the endothelial production of NO catalyzed by NOS3 is ignored here, as described in *Model assumptions*. In the intraluminal layer (layer 1), NO reacts with oxygen in the plasma, and no NO source exists in this subregion. Inside RBCs, NO (or nitrosonium) bound to the cysteine residue of Hb β chains is transferred to the thiols on the anion exchange protein, which is attached to the membrane (40). These NO_x are then exported from the cell. We model this process as a surface release determined by the apparent half-life and concentration of SNOHb, ignoring the intermediate processes. This facilitated release is unidirectional: the NO molecules that are released will encounter transport resistance when they diffuse back into the RBCs. This resistance can be specified by a high diffusivity in the thin membrane sublayer that is related to the measured membrane permeability (10). When NO diffuses back into the RBCs, it will rapidly react with the intraerythrocytic Hb.

Layer 1 contains two subregions: the plasma and RBCs. In each RBC, NO is consumed through hemoglobin scavenging:

$$R_{NO} = -k_{Hb} C_{Hb} C_{NO} \quad (2)$$

where k_{Hb} is the kinetic reaction rate between Hb and NO, C_{Hb} is the hemoglobin concentration, and C_{NO} is the NO concentration. A thin sublayer along an RBC was created to represent the RBC membrane, which possesses an intrinsic resistance to NO diffusion. The NO on the β93-cysteine of hemoglobin is transferred to the membrane-bound protein (band 3 protein), and then is released outside the RBC. The release rate of this

process is modeled as a surface reaction and expressed as a boundary flux, as discussed later. Meanwhile, in the plasma subregion, NO can freely diffuse in any direction. Also, the chemical reaction in the plasma subregion is expressed as:

$$R_{NO} = -k_{O_2} C_{O_2} C_{NO}^2 \quad (3)$$

where k_{O_2} is the kinetic reaction rate between oxygen and NO, and C_{O_2} is the oxygen concentration.

In layer 2, the NO production catalyzed by NOS3 is ignored; NO is consumed through reactions with oxygen:

$$R_{NO} = -k_{O_2} C_{O_2} C_{NO}^2 \quad (4)$$

In layer 3, NO is consumed through reactions with sGC:

$$R_{NO} = -k_{sGC} C_{NO}^2 \quad (5)$$

where k_{sGC} is the kinetic reaction rate between sGC and NO.

In layer 4, the possible NO production by NOS1 is ignored; NO is consumed through the reactions with oxygen:

$$R_{NO} = -k_{O_2} C_{O_2} C_{NO}^2 \quad (6)$$

In layer 5, NO is consumed through reactions with oxygen and hemoglobin contained in RBCs flowing through the capillaries in the capillary-perfused region. Thus, the net reaction in this layer is

$$R_{NO} = -k_{O_2} C_{O_2} C_{NO}^2 - k_{cap} C_{NO} \quad (7)$$

where k_{cap} is the effective reaction rate between NO and cellular hemoglobin in the capillaries.

Parameter values

In the present study, we modeled the NO profile around an arteriole and surrounding tissue. In our calculations, we chose 4 μm as the effective radius of an RBC (r_1), which was modeled as a circle. The thickness of the RBC membrane (r_{mem}) was chosen as 0.0078 μm (49), and the radius of the precapillary arteriolar lumen (r_3) was chosen as 17 μm. When the RBC-free layer was considered, we used a value of 2 μm, which resulted in a region with a radius of 15 μm (r_2) that contains RBCs. The radius (r_4) chosen for the endothelium and interstitial space layer was 18 μm, with an assumption that the thickness of the endothelium and interstitial space was 1 μm. The thickness of the smooth muscle was considered to be 6 μm (17), making the radius (r_5) of the outer edge of the smooth muscle layer 24 μm. The thickness of the nonperfused tissue was considered to be 6 μm, resulting in 30 μm as the radius (r_6) of the nonperfused tissue layer. Finally, the radius (r_7) of the entire region was considered to be 50 μm, with a choice of 20 μm as the thickness of the perfused tissue.

As stated earlier, a 45% hematocrit was chosen as a reference value (39), and this value determined how many RBCs were placed in the lumen. The diffusivity of NO was 3,300 $\mu m^2/s$ in all regions except within the RBCs (50). Inside the RBCs, NO diffuses less rapidly than in the extracellular space, with a diffusivity of 880 $\mu m^2/s$ (49). The intracellular concentration of hemoglobin heme (C_{Hb}) was 20 mM, and the reaction rate (k_{Hb}) between Hb and NO was 18 $\mu M^{-1}s^{-1}$ (5). The concentration of sGC (C_{sGC}) was 0.1 μM, and the reaction rate between sGC and NO (k_{sGC}) was 0.05 $\mu M^{-1}s^{-1}$ (50). The effective reaction rate between NO and the capillary hemoglobin (k_{cap}) was 12.4 per s, as justified in (26). The reaction rate between oxygen and NO was 9.6×10^{-6} $\mu M^{-2}s^{-1}$ (26). Also, the concentration of ambient oxygen as a reactant had little impact on the NO profile (see Results), and therefore we set C_{O_2} to 0 unless otherwise indicated.

The release rate of NO depends on the concentration of RBC-bound NO and the half-life of SNOHb *in vivo*. The amount of circulating SNOHb in the blood has been under debate because of methodologic inconsistencies (33). A wide range of concentrations for SNOHb has been reported, from subnanomolar (35) to 46–49 nM (14) to >300 nM (40) and >20 μM (21). Rogers *et al*. (37), by using an enhanced triiodide reagent that avoids the autocapture of NO by heme, reported a concentration of 445–600 nM RBC-bound NO in venous blood, which was equivalent to an intracellular SNOHb concentration of 989–1,333 nM, assuming a 45% hematocrit and that all the measured RBC-carried NO was bound to the hemoglobin β chains. However, the assay used in (37) may lack the specificity for *S*-nitrosothiols, as recently reviewed by MacArthur *et al*. (33). MacArthur *et al*. also pointed out that SNOHb concentration was around 50 nM. In the present study, we used 1,333 nM, the upper value of the reported range by Rogers *et al*. (37), as the SNOHb concentration; we also calculated the NO bioavailability with 50 nM SNOHb present. Moreover, we varied this parameter to test the sensitivity of the NO distribution. The half-life of SNOHb *in vivo* has been reported to be 240 s in room air (41). This parameter was also varied to test the sensitivity of the NO distribution. Thus, the NO release rate from the RBC is determined by (19):

$$Q_{NO} = C_{SNOHb} \cdot \ln \frac{2}{t_{1/2}}$$

where Q_{NO} is the apparent volumetric NO production rate based on the whole volume of an RBC, C_{SNOHb} is the intracellular concentration of SNOHb, and $t_{1/2}$ is the half-life of SNOHb. By using 1,333 nM as C_{SNOHb} and 240 s as $t_{1/2}$, we obtained Q_{NO} = 3.85 nM/s. This volumetric NO production rate was converted to a surface release rate, as shown later.

According to the SNOHb hypothesis, the NO group on the β-93 cysteine can be transferred to membrane-associated proteins and then further exported out of the cell. Thus, the NO group can avoid being scavenged through rapid rebinding to the hemoglobin iron. In our model, we represented this series of biochemical reactions by using an apparent surface-release reaction. The total amount of the released NO is the product of the volume of a RBC (V) and the NO production rate (Q_{NO}; determined earlier). Thus, the surface-release rate of NO from the RBC membrane per unit time per unit area is

$$S_{NO} = \frac{Q_{NO} \cdot V}{A}$$

where A is the surface area of the RBC. Both V and A are determined by the radius of the RBC. Given the values of Q_{NO} and the radius of RBC in Table 1, S_{NO} is 5.13×10^{-18} $\mu mol/\mu m^2/s$.

TABLE 1. MODEL PARAMETERS

Parameters	*Value/unit*	*Reference*
Radius		
RBC (r_1)	4 μm	(10, 49)
RBC-rich layer (r_2)	15 μm	text
RBC-free layer (r_3)	17 μm	text
Endothelium and interstitial space (r_4)	18 μm	text
Smooth muscle layer (r_5)	24 μm	text
Nonperfused tissue (r_6)	30 μm	text
Perfused tissue (r_7)	50 μm	text
RBC membrane thickness (r_{mem})	0.0078 μm	(10, 49)
RBC membrane permeability (P_{RBC})	450 μm/s	(10, 49)
NO diffusion coefficient in membrane (D_{mem})	3.51 $\mu m^2/s$	text
Extracellular NO diffusion coefficient (D_{ext})	3,300 $\mu m^2/s$	(50)
Intracellular NO diffusion coefficient (D_{int})	880 $\mu m^2/s$	(49)
Hb-NO reaction rate (k_{Hb})	18 $\mu M^{-1}s^{-1}$	(5)
Intracellular Hb concentration (C_{Hb})	20 mM	text
Reaction rate with sGC (k_{sGC})	0.05 $\mu M^{-1}s^{-1}$	(50)
Oxygen concentration (C_{O2})	0–100 μM	text
Reaction rate with O_2 (k_{O2})	9.6×10^{-6} $\mu M^{-2}s^{-1}$	(26)
SNOHb concentration (C_{SNOHb})	1,333 nM	(37)
SNOHb half-life ($t_{1/2}$)	240 s	(41)
NO surface release rate (S_{NO})	5.13×10^{-18} μmol/μm^2/s	text
NO consumption rate by perfused tissue (K_{cap})	12.4 per second	(26); text

The radius of each layer, except r_1, represents the distance from the center of the lumen to the outer boundary of the layer.

The production of NO by the RBC-NO was incorporated as surface NO release into the boundary conditions at the interface between the RBC membrane and the plasma (see later).

Boundary conditions

All boundaries between the regions described in the *Model geometry* section have continuous NO-concentration distributions, except for the interface between the RBC membrane and the plasma, where a finite transport resistance is introduced. At the outer interface of the whole region, we assume a no-flux condition. The boundary conditions are

1. At the outer boundary of layer 5:

$$\frac{\partial C_{NO}}{\partial r} = 0 \tag{8}$$

2. At the interface between the plasma and the RBC, the NO release from the RBC is incorporated as the surface boundary condition:

$$S_{NO} = D_{NO,mem} \frac{\partial C_{NO,mem}}{\partial r} - D_{NO,plasma} \frac{\partial C_{NO,plasma}}{\partial r} \tag{9}$$

where S_{NO} is the NO release from the RBC surface through the band 3 protein mechanism, $D_{NO,mem}$ is the diffusivity of NO in the RBC membrane, $D_{NO,plasma}$ is the diffusivity of NO in the plasma, $C_{NO,mem}$ is the NO concentration in the thin RBC membrane layer, and $C_{NO,plasma}$ is the NO concentration in plasma. In the membrane of each RBC, the apparent diffusivity of NO was determined by the membrane permeability (P_{mem}) and the membrane thickness (r_{mem}) (10):

$$D_{NO,mem} = P_{mem} \cdot r_{mem} \tag{10}$$

The values used for parameters P_{mem} and r_{mem} are 450 μm/s and 0.0078 μm, respectively (10, 49). Thus, the apparent diffusivity of NO inside the RBC membrane is 3.51 $\mu m^2/s$. In our numerical calculations, we used a larger r_{mem} (0.078 μm, a value still much less than the RBC size) and thus higher $D_{NO,mem}$ (35.1 $\mu m^2/s$) to make our numeric solutions more efficient. To ensure that the approximation was valid, we calculated the NO distribution under the conditions described in Fig. 2E by using both values of r_{mem} described earlier (and thus both $D_{NO,mem}$) and found that the calculated results were the same (data not shown).

Numeric method

The governing equation (Eq. 1) coupled with the appropriate boundary conditions was solved numerically by using the FlexPDE software package (PDESolutions, Antioch, CA). The code was implemented on a 3-GHz processor with 2 GB synchronous dynamic random access memory (SDRAM).

RESULTS

The NO concentration in smooth muscle

We first calculated the NO-concentration distribution around an arteriole when intraerythrocytic SNOHb was the sole source of NO (Fig. 2). The calculations were performed with four different distributions of RBCs inside the lumen (A–D), with a 45% hematocrit. Despite the different positions of the intraluminal RBCs, all four simulations showed a concentration of ~6 pM NO in the vascular smooth muscle region. Inside the lumen, the concentration of NO in the intercellular regions was

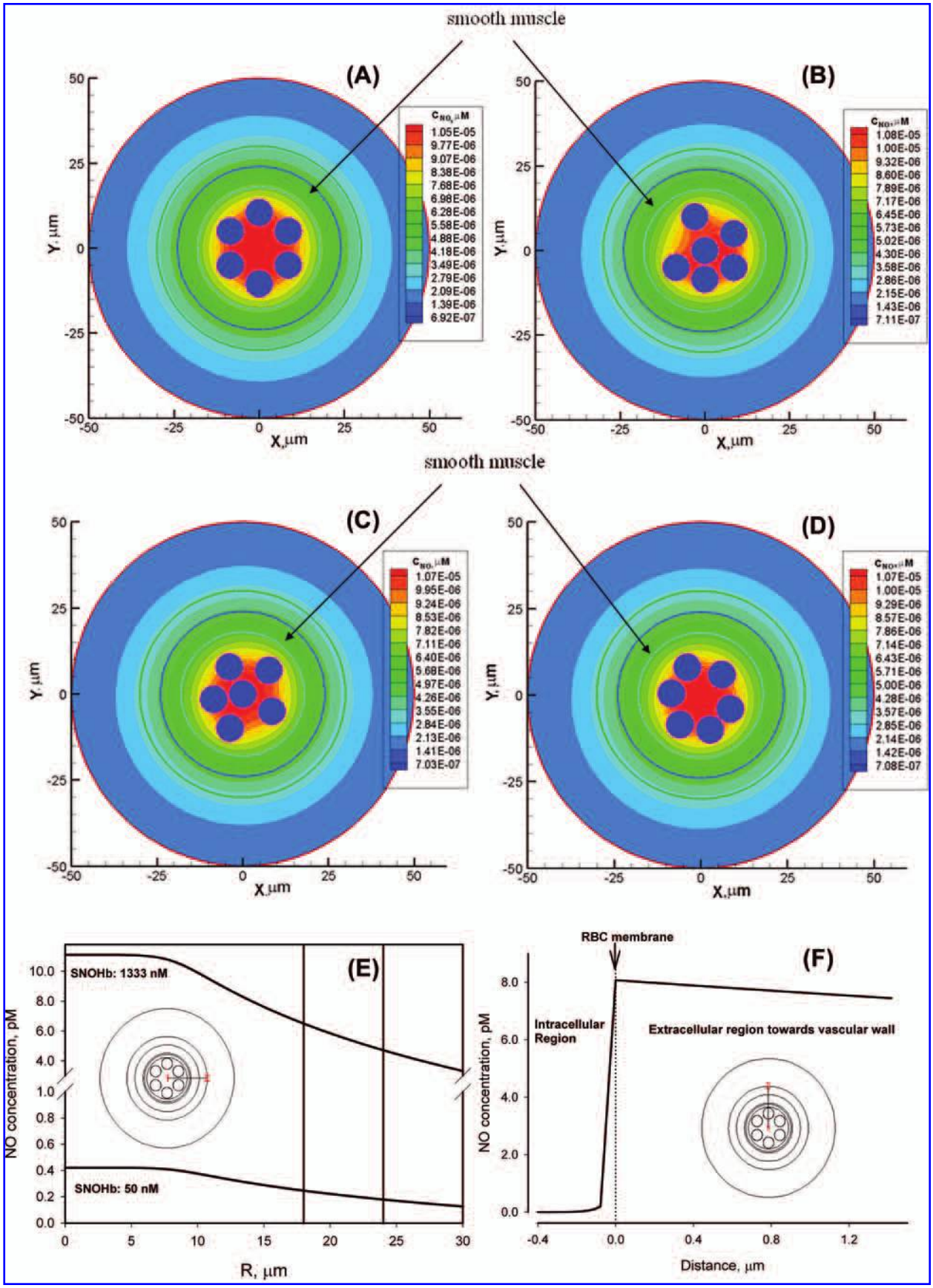
smooth muscle
(A)
(B)
smooth muscle
(C)
(D)
Y, μm
X, μm
(E)
SNOHb: 1333 nM
SNOHb: 50 nM
NO concentration, pM
R, μm
(F)
RBC membrane
Intracellular Region
Extracellular region towards vascular wall
NO concentration, pM
Distance, μm

~10 p*M* NO, whereas the NO concentration inside the RBCs was significantly lower, apparently because of the strong scavenging effect by intracellular hemoglobin. Also, Fig. 2A–D shows a minimal influence of RBC positioning on the NO concentration of the vascular wall. Thus, for the sake of simplicity, we focused on the distribution of RBCs in Fig. 2A in our subsequent calculations. Note that all calculations in Fig. 2A–D were based on the intraerythrocytic SNOHb concentration of 1,333 n*M*.

Figure 2E shows representative plots of NO concentration along a path (Fig. 2E, inset) from the center of the lumen to the surrounding tissue. The upper curve shows that the NO concentration was 4.7–6.5 p*M* in the smooth muscle region with 1,333 n*M* SNOHb in erythrocytes. Whether this predicted ~6 p*M* concentration is sufficient to activate sGC for vasodilation is discussed later. The amount of NO released would be significantly reduced if SNO-Hb levels in erythrocytes are in the 50 n*M* range, a value reported by several other groups (33), rather than the 1,333 n*M* reported by Rogers *et al*. (37). Figure 2E also shows that NO bioavailability in smooth muscle is predicted to be ~0.25 p*M* when SNOHb level is as low as 50 n*M*.

Figure 2F shows the NO concentration gradient across the RBC membrane. After being released from the RBC through the facilitated mechanism, NO molecules can diffuse back into the cell. NO is scavenged by hemoglobin once it diffuses back, and the intracellular concentration of NO rapidly decreases to nearly zero from the higher concentration close to the membrane. Thus, a significant amount of NO released from RBCs is still consumed by intracellular hemoglobin. We estimated that the net ratio of NO diffusing out of RBCs is ~17% (see Discussion).

NO concentration as a function of SNOHb concentration and the half-life of SNOHb

As shown earlier, the NO release rate from SNOHb is critically dependent on the concentration and the half-life of SNOHb. These two parameters may vary with changes in hemoglobin oxygen saturation (41). Thus, we tested the NO exposure of smooth muscle as a function of these two parameters. Because a concentration gradient of NO was found in the smooth muscle region, we compared the NO concentration at the inner boundary of the smooth muscle layer for all simulations with different SNOHb concentrations or $t_{1/2}$ parameter. Figure 3A shows that the NO exposure of smooth muscle increased linearly with increasing SNOHb concentration; Figure 3B shows that, given a specific SNOHb concentration, the NO availability in the smooth muscle is negatively related to $t_{1/2}$. Thus, NO delivered by SNOHb to smooth muscle is strongly dependent on these two parameters.

The effect of O_2 on NO availability

Ambient O_2 may affect the NO distribution through the reaction that occurs once NO is released from RBCs. In our previous calculations, we used a value of 0 for the O_2 concentration to represent hypoxic conditions. We also calculated the NO availability with other O_2 levels from 0 to 100 μM with a fixed NO-release rate from RBCs. We found that the NO distribution around the arteriole was essentially constant for the various O_2 concentrations tested (data not shown). This result indicates that the reaction between NO and O_2 has little influence on the NO distribution. It should be noted that, although O_2 was not a significant scavenger for NO, the NO-release rate from either enzymatic or nonenzymatic sources is sensitive to different oxygen tensions (40); enzymatic sources were not considered in the present study.

NO distribution as a function of RBC membrane permeability

After the NO was released by RBCs through a facilitated mechanism (2, 40), the released NO could diffuse toward the smooth muscle target or back into the RBCs. Initially, it was thought that NO can freely diffuse through the plasma membrane of RBCs (31), but recent studies have shown that the membrane possesses an intrinsic resistance to NO diffusion (4, 10), which is important for the paracrine NO regulation of vascular tone. We tested how the membrane resistance (or the membrane permeability to NO) affects the NO exposure of the smooth muscle. Figure 4 shows that when the membrane permeability was 1 μm/s, a level of 39 p*M* NO would be present in the smooth muscle region. With higher membrane permeability, less NO would be available, because the more resistant membrane can prevent the scavenging of NO by the intracellular hemoglobin once the NO is released into the intercellular space of the lumen.

We also calculated the NO distribution in the case of a membrane permeability of 423,076 μm/s. This value corresponded to an apparent diffusion coefficient of 3,300 μm^2/s with a

FIG. 2. NO concentration profile around an arteriole. Cross sections of an arteriole and its surrounding tissues. RBC-released NO was the sole source of NO. RBCs were inside the lumen. Four different distributions of intraluminal RBCs (**A–D**) were simulated. All parameters are listed in Table 1. Hematocrit was 45%, and the oxygen concentration was set to 0 to mimic hypoxic conditions. The NO concentration inside each RBC was nearly zero. Despite different RBC positioning in the lumen, the NO concentrations around the arteriole were similar. (**E**) NO concentration distributions along a path from the center of the lumen to the outer edge of the nonperfused tissue layer. In addition to the condition when SNOHb concentration was 1,333 n*M*, the NO concentration profile also was calculated when the SNOHb concentration was 50 n*M*. The circles in the inset represent RBCs. The specific path is shown in the inset, and the starting and ending points are presented as 1 and 2, respectively. The marked region represents the smooth muscle layer. (**F**) NO concentration gradient across cell membrane of one simulated RBC. The gradient is along a path crossing the center of the RBC (inset). Because of the steep gradient close to the cell membrane inside the RBC, we plotted the concentration in a short distance (from the intracellular point 0.4 μm to the membrane, to the extracellular point 1.4 μm to the membrane) to have a better viewing effect. The zero position in the x-axis represents the outer edge of the membrane at the path shown in the inset. NO concentration rapidly decreases to nearly zero in the intracellular region. (For interpretation of the references to color in this figure legend, the reader is referred to the web version of this article at www.liebertonline.com/ars)

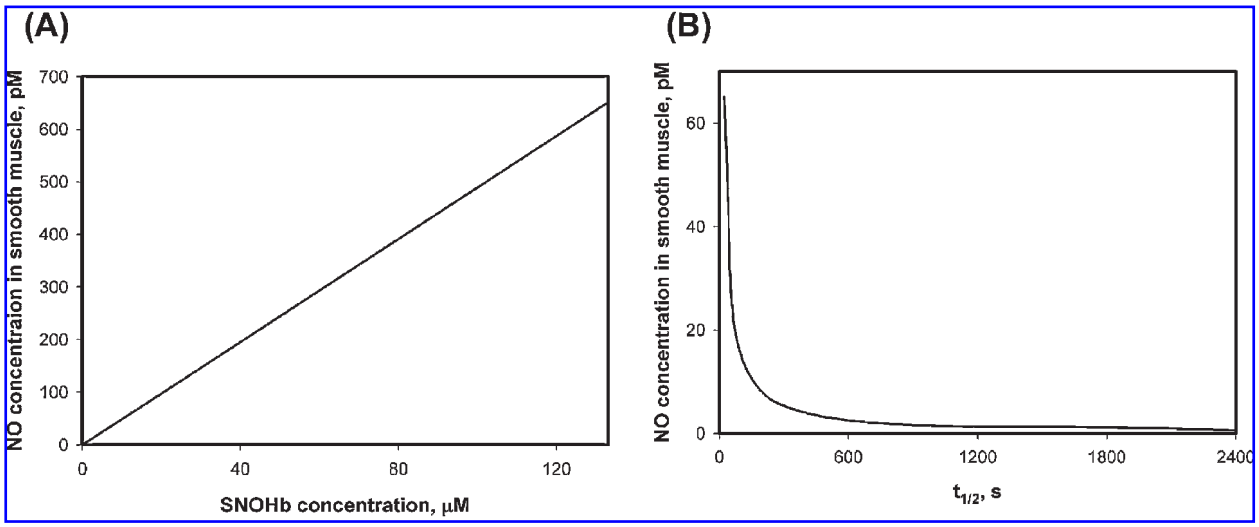

FIG. 3. The NO concentration in smooth muscle as a function of (A) the concentration of SNOHb or (B) the half-life of SNOHb. The RBC distribution and other simulation conditions are the same as those shown in Fig. 2A. The NO concentrations shown in the figure are the values at the inner boundary of the smooth muscle region. In (**A**), the half-life of SNOHb was fixed at 240 s. In (**B**), the SNOHb concentration was fixed at 1,333 n*M*.

0.0078-μm membrane thickness (Table 1), indicating that no additional resistance to NO diffusion through the membrane was present. As shown in Fig. 4, this calculation yielded a 0.2 p*M* concentration for NO in the smooth muscle region, a value 33-fold lower than that with the reported membrane permeability (Fig. 2). This difference suggests that the resistance of the RBC membrane has a significant influence on the endocrine NO release.

NO concentration as a function of hematocrit

The influence of the hematocrit on the delivery of NO to the smooth muscle was also tested by varying the hematocrit from 7 to 60%. The results showed that the higher the hematocrit, the larger was the concentration of NO present in the smooth muscle. With a 7% hematocrit, the NO concentration in smooth muscle was ~2.8 p*M*, whereas with a 60% hematocrit, the NO concentration was ~6.7 p*M*, a 2.4-fold increase. The NO concentration was not linearly proportional to the change in hematocrit, suggesting that the change in hematocrit under physiologic conditions (<20% change) would not produce a relatively large variation in exposure of the smooth muscle to NO.

Influence of the RBC-free region

The RBC-free layer has been found to be an important gap that reduces the effective scavenging of endothelium-derived NO and, as a result, preserves a substantial amount of paracrine NO that can migrate to the vascular smooth muscle (6). To this point, in our model, we used a 2-μm-thick region that did not contain RBCs. To test the role of this layer in NO signaling in the endocrine-regulation scenario, we calculated the NO deliv-

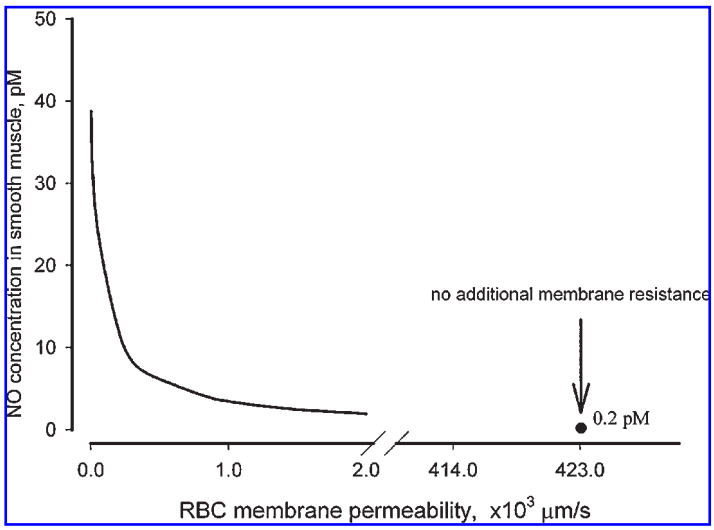

FIG. 4. Influence of the membrane permeability of a RBC on the delivery of NO to smooth muscle. The curve represents the variation in RBC membrane permeability, from 1 to 2,000 μm/s. The dot point in the plot represents the NO concentration when the membrane does not have additional resistance to the transport of NO (a membrane permeability resulting in a diffusion coefficient the same as that in the plasma). All other conditions of the simulation experiments were the same as those in Fig. 2A. The NO concentration in the inner boundary of the smooth muscle is plotted.

ery by RBCs when the cells were distributed quite near to the vascular wall, effectively eliminating the RBC-free layer (Fig. 5B). For comparison, Fig. 5A shows the NO distribution when RBCs are distributed mainly in the central region of the lumen. In both cases, the hematocrit was 45%. We found that the NO concentration at the inner boundary of the smooth muscle was 6.7 p*M* (Fig. 5A and C) when most of the RBCs were near the center of the lumen, whereas it was 7.2 p*M* (Fig. 5B and C) when most of the RBCs were close to the vascular wall (no RBC-free layer near the wall), a 7% increase. Figure 5C shows the difference in the NO concentration along a specific path.

NO concentration when endothelium-derived NO also is considered

In our simulations, we considered the NO delivery when the NO released from RBCs was the sole source in the vasculature. Now we calculated the NO concentration profile when the enzymatic NO production from NOS3 is also included in the model. The reported NO production rate covers a large range (5, 7). Here we used a small production rate (0.017 μm/s) based on our previous biochemical pathway analysis of NOS3 catalysis. The calculated NO concentration profile (Fig. 6) shows

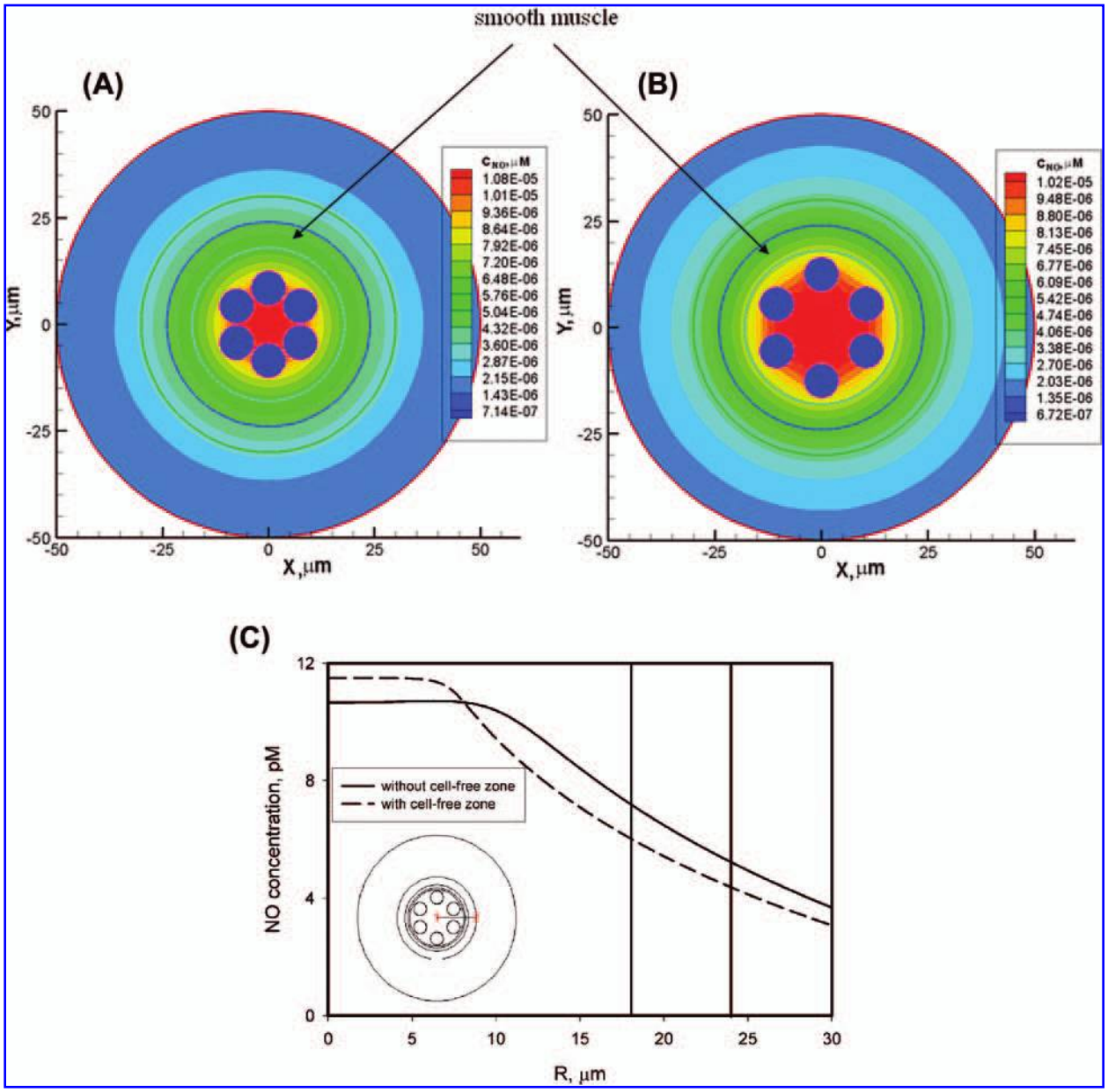

FIG. 5. The NO-concentration distributions when the cell-free layer is considered (A) and not considered (B). Other simulation conditions are the same as those in Fig. 2A. A typical NO-concentration distribution along a path from the center of the lumen to the outer edge of the nonperfused tissue layer is shown. The specific path is shown in the inset in (**C**) and the starting and ending points are presented as 1 and 2, respectively. The marked region represents the smooth muscle layer. (For interpretation of the references to color in this figure legend, the reader is referred to the web version of this article at www.liebertonline.com/ars)

that the NO concentration in smooth muscle region is ~47 p*M*. This value is still significantly lower than the values measured *in vivo* (47, 51, 53). Moreover, because the NO production rate by the endothelium is still significantly higher than that from RBCs and because the RBC-released NO is closer to the scavengers (hemoglobin), the enzymatic NO contributes more than SNOHb to smooth muscle NO exposure in this simulation.

DISCUSSION

We used a multicellular computational model to quantify the NO exposure of smooth muscle when the endocrine release of NO by RBCs under hypoxic conditions was the sole source of NO in the vasculature. We also tested the impact on NO distribution of certain parameters, including the SNOHb concentration, the half-life of SNOHb, the ambient O_2 concentration, the hematocrit, the membrane resistance to NO free diffusion, and the existence of an RBC-free layer. The parameters that significantly influenced the vasodilation by the RBC-released NO could be identified from the simulation tests.

Comparison of our model predictions with the results of previous studies

Because of the high sensitivity and specificity required for NO detection, no direct quantitative *in vitro* or *in vivo* experimental measurements of NO released by RBCs have been made. Jeffers *et al*. (22) used a mathematical model to quantify the NO that reached smooth muscle when intracellular nitrite was reduced by hemoglobin to become NO. In their model, ~8 p*M* NO would be present in smooth muscle, provided an intermediate species process that possessed a longer half-life was available during the nitrite-reduction. This value of 8 p*M* is close to that predicted from our model (~6 p*M*, Fig. 2), although both models will need to be tested experimentally when more precise experimental techniques are developed.

Is the RBC-released NO sufficient to activate sGC?

The answer to this question depends on how much NO is required to achieve half-maximal activity of sGC (*e.g*., EC_{50} of NO). Stone and Marletta (42) showed that at least 250 n*M* NO was required to stimulate half-maximal activity of sGC at 10°C. This value was reduced to 23 n*M* in a later study by Condorelli and George (9). Recent reports suggested that the EC_{50} of NO is in the low nanomolar range (12, 38). Moreover, as discussed in ref. 7, 20–100 p*M* NO present in smooth muscle may be able to trigger maximal vascular relaxation through a mechanism that does not require the full potential of cGMP accumulation achievable by full cyclase activation, as suggested in the study by Kollau *et al*. (29). Thus, whether the delivery of 6 p*M* NO by SNOHb to vascular smooth muscle is sufficient for vasodilation depends on a more clear investigation into the EC_{50} of NO. Moreover, smooth muscle could relax if a higher concentration of SNOHb is present in RBCs, the synthesis of SNOHb utilizing nitrite can supply a higher level of SNOHb under hypoxic conditions (3), or NO can be released from other intraluminal reservoirs (*e.g*., nitrite).

Another possibility is that the RBC-released NO supplements the enzymatically generated NO under hypoxic conditions. The NO production catalyzed by NOS is expected to decrease during hypoxia (8). As a result, the exposure of smooth muscle to the enzymatically generated NO may be below the EC_{50} value, and thus the delivery of NO by SNOHb would become an important supplementary source for inducing vessel relaxation.

Two problems need to be addressed with this scenario. First, the predicted values of the NO concentration are orders of magnitude lower that those perivascular values measured *in vivo* with NO microelectrodes; these values have been reported in the range of 200–600 n*M* under control conditions, as described in greater detail later. Second, if the EC_{50} is indeed as low as quoted earlier (several nanomolar), and the perivascular NO concentration is in the range of several hundred nanomolar, then how is the vasculature regulated? At present, these questions remain unresolved.

Sensitive parameters determining NO bioavailability

We tested the effect in our model of various parameters that potentially have an influence on NO bioavailability. A higher concentration (Fig. 3A) or shorter half-life (Fig. 3B) of SNOHb (provided that the consumed SNOHb can be quickly replenished) can significantly improve NO delivery. Conversely, hematocrit and ambient O_2 do not strongly affect the distribution of NO released by RBCs. The existence of a cell-free region, or whether RBCs are near the vascular wall, has been postulated to play an important role in RBC-delivered NO (36). Our calculations have shown that these variables do not significantly affect the NO delivery (7% change; Fig. 5), although the cell-free region was important as a barrier to protect enzymatic NO from being effectively scavenged by RBCs. Another sensitive parameter in terms of NO delivery by SNOHb was the membrane permeability of the RBC to NO, as discussed later.

RBC membrane resistance to NO diffusion

NO, an uncharged small molecule, was initially thought to be able to diffuse freely through the RBC membrane (31). However, the fact that most paracrine NO would be consumed by intraluminal hemoglobin has led researchers to question whether the RBC membrane can provide a barrier to alleviate NO scavenging by the encapsulated hemoglobin. Competition experiments in combination with a distributed multicellular model (4, 49, 50) have shown that the RBC membrane does indeed possess an intrinsic resistance to NO diffusion, a mechanism that supports the paracrine regulation of NOS-derived NO. Figure 4 shows that this membrane barrier (as represented by membrane permeability) can reduce the quenching of NO bioactivity that is released by the RBC itself, enhancing endocrine delivery. If no membrane resistance existed, NO delivery by RBCs to smooth muscle would be more than 30-fold lower than

that calculated by using the reported permeability (Fig. 4). Thus, the RBC membrane possesses an intrinsic barrier that is essential to both paracrine and endocrine regulation of vascular tone by NO.

Effect of the facilitated membrane release mechanism

The endocrine regulation of vascular tone by intraerythrocytic SNOHb is based on a hypothesis that the NO molecule carried by hemoglobin is released through a facilitated transport mechanism involving the anion-exchange protein on the membrane *via* transnitrosation (2, 40). This or a similar NO-release mechanism appears to be necessary, because otherwise the released NO would be strongly scavenged by intracellular hemoglobin. We were able to use our model to justify how much NO would be able to reach the smooth muscle if such a mechanism did not exist. We modified our model by considering a uniform NO production inside RBCs, rather than a flux of NO on the RBC surface that resembles the facilitated NO release. A $Q_{NO} = C_{SNOHb} \cdot \ln \frac{2}{t_{1/2}} = 3.85$ nM was considered inside each RBC, and a continuous NO-concentration distribution was preserved at the interface of the outer boundary of the RBC membrane and the plasma. All other conditions were unchanged. The calculations showed (Fig. 7) a smooth muscle concentration of only 5.5×10^{-3} pM NO, a value nearly three orders of magnitude smaller than that in Fig. 2. As discussed earlier, the picomolar level of NO may be able to activate sGC for hypoxic vasodilation, but a value 1,000-fold lower would be too small to have any physiologic significance. Taken together, these results indicate that facilitated transport of NO or NO equivalents through the RBC membrane is essential for endocrine regulation by the RBC-released NO.

Does the SNOHb-carried NO account for the perivascular NO measurements?

Periarteriolar measurements have shown several hundred nanomolar NO around arterioles, and the measured values cover a relatively large range. Bohlen and colleagues (34, 53) reported perivascular NO level of ~500 nM in their measurements in intestinal arterioles of Sprague–Dawley rats. Vukosavljevic *et al*. (51) reported a perivascular NO concentration of 300–400 nM in mesentery and intestine in the same animal model. The values reported for the dorsal skin of golden Syrian hamsters were 200 and 600 nM in the experiments by Tsai *et al*. (46, 47). However, our theoretic analyses of the biochemical pathways of NOS1 and NOS3 showed large discrepancies between the model predictions of enzymatic NO levels and the perivascular NO measurements (7, 8). One of the primary goals of this study was to investigate whether RBC-released NO can account for these discrepancies. Apparently, they cannot. Other enzymatic or nonenzymatic sources of NO in the perivascular region are more likely to account for the measured values. Analyses of alternative pathways leading to NO release are needed; at present, NOS3 expressed on the RBC membrane (28) and the putative mtNOS may be the potential sources that contribute to the perivascular NO measurements.

Limitations of the model

In the model-formulation section, we assumed that the released nitrosonium was in the form of free NO. This assumption may not be accurate, because the released NO bioactivity may be present in the form of other small molecules, such as *S*-nitrosoglutathione (GSNO). In such a case, the released species may be considerably less reactive with hemoglobin and cause a vasoactive effect directly, or the subsequent liberation of NO from this species occurs only in the vascular wall. To predict the concentration of this species in the smooth muscle, the governing equation (Eq. 1) must be modified (*i.e.*, the diffusion coefficient, reactivity with other species present in the vasculature, and permeability of the membrane must be adjusted). Other forms of protein molecules carrying a nitrogen oxide group are likely to have smaller diffusion coefficients and to be less reactive than free NO. Considering that the scavenging of NO by oxygen in the arteriolar lumen is already insignificant (see Results), we do not expect that the diffusivity and reactivity of molecules carrying NO bioactivity in the extracellular space in the lumen would have a significant impact on the NO concentration in the smooth muscle. With extremely low cell-membrane permeability, the released molecules that carry NO bioactivity would effectively avoid the reactions with intraerythrocytic hemoglobin. We modified the model by setting the membrane permeability to 0.001 μm/s (further decrease in this parameter did not affect the calculated NO concentration profile) and predicted 39.3 pM of this released species present in smooth muscle. Compared with the 6.7 pM NO with 450 μM/s membrane perme-

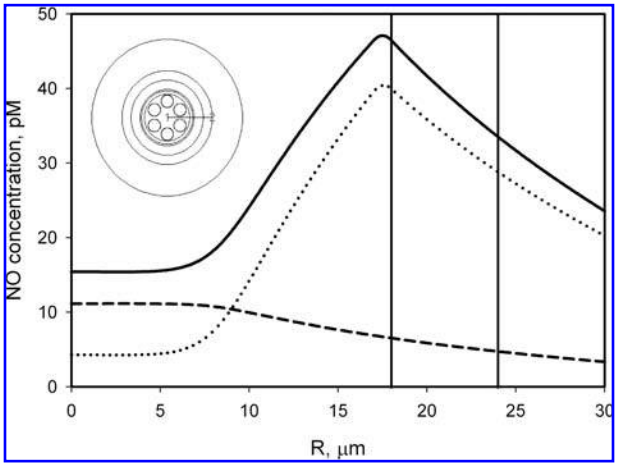

FIG. 6. NO-concentration profile around an arteriole when RBC-released NO and endothelium-released NO were the NO sources (*solid line*), endothelium-released NO was the only source (*dotted line*), and RBC-released NO was the only source (*dashed line*). The NO-production rate from the endothelium was 0.017 μm/s (7). All other information is the same as that in Fig. 2E. NO-concentration distributions along a path from the center of the lumen to the outer edge of the nonperfused tissue layer are shown. The specific path is shown in the inset, and the starting and ending points are presented as 1 and 2, respectively. The marked region represents the smooth muscle layer.

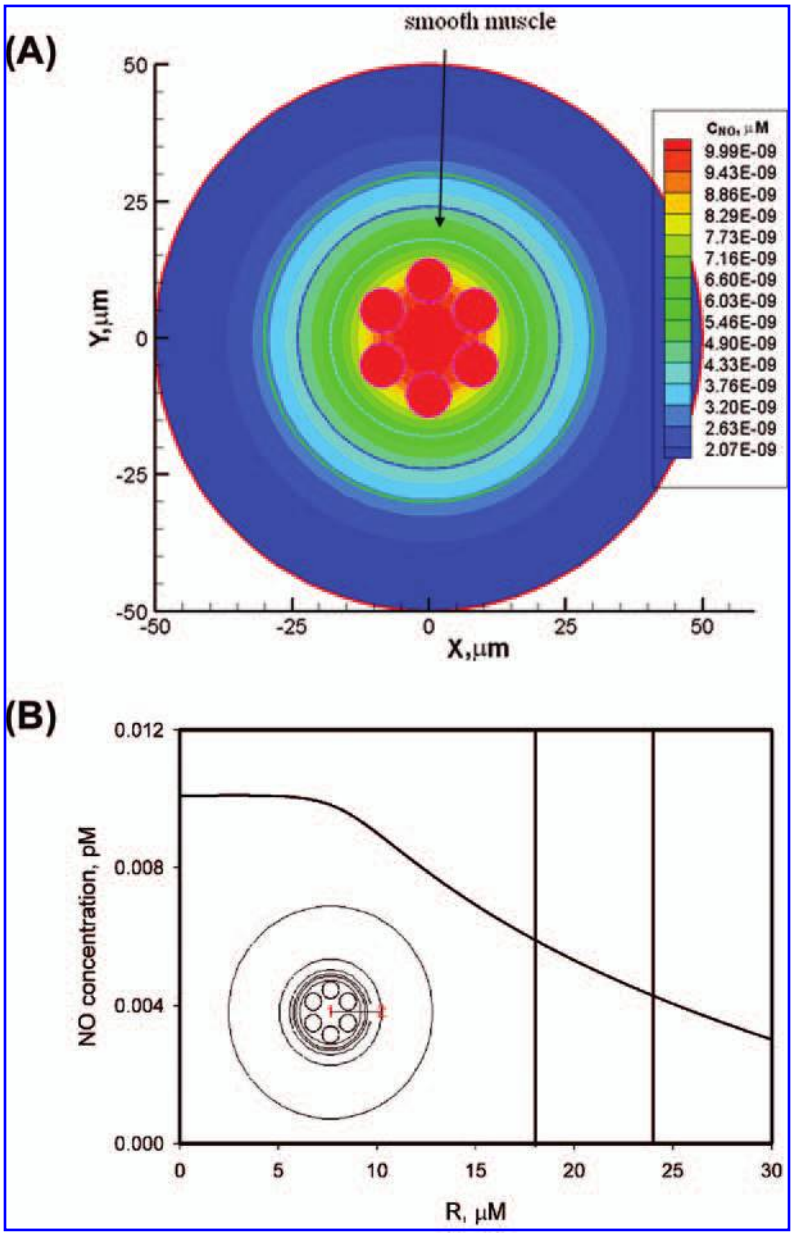

FIG. 7. NO-concentration profile around an arteriole when no facilitated mechanism exists for NO release through the membrane. All other simulation conditions are the same as those in Fig. 2A. (**A**) The NO-concentration profile. (**B**) A typical NO-concentration distribution along a path from the center of the lumen to the outer edge of the nonperfused tissue layer. The specific path is shown in the inset in (**B**), and the starting and ending points are presented as 1 and 2, respectively. The marked region represents the smooth muscle layer. (For interpretation of the references to color in this figure legend, the reader is referred to the web version of this article at www.liebertonline.com/ars)

ability, the net ratio of NO diffusing out of RBCs is ~17%. Thus, we estimated that the presence of the molecules carrying NO bioactivity would be ~39 p*M*. More precise calculations can be made when the mechanism of the released NO bioactivity is determined.

We also used a constant SNOHb concentration in our model, with the assumption that the SNOHb consumption could be replenished by flow, NO rebinding, and synthesis by converting other nitrogen oxide species. During the RBC-controlled hypoxic vasodilation, the concentration of SNOHb may change over time. A more detailed study of these kinetic processes is needed to provide a more accurate prediction of NO delivery by SNOHb. In addition, we used a two-dimensional model representing RBCs and the cross sections of an arteriole, as well as its associated tissue. This model underestimates the surface-to-volume ratio of real three-dimensional RBCs. The NO delivered by the intraerythrocytic SNOHb to the vessel wall could be slightly higher than the predictions in our two-dimensional model but should be far below the discrepancies that we have encountered (discussed earlier).

CONCLUSIONS

We have predicted that the amount of NO delivered by intraerythrocytic SNOHb to the vascular wall is in the neighborhood of 6 p*M* under the SNOHb hypothesis; this NO availability would be as low as 0.25 p*M* if the SNOHb concentration is 50 n*M*, as reported in some studies. The NO released by SNOHb, especially if SNOHb level is at 50 n*M*, appears not sufficient alone to induce the hypoxic vasodilation. The amount

of NO present in the smooth muscle depends strongly on facilitated membrane transport, membrane resistance to NO diffusion, and the physiologic level and half-life of SNOHb. The predicted values of vascular smooth muscle NO concentration are several orders of magnitude lower than the measured perivascular values.

ACKNOWLEDGMENTS

This research was supported by NIH grants R01 HL018292 and R01 HL079087.

ABBREVIATIONS

GMP, 3′,5′-cyclic guanosine monophosphate; Hb, hemoglobin; NO, nitric oxide; NOS, nitric oxide synthase; NOS1, neuronal NOS; NOS2, inducible NOS; NOS3, endothelial NOS; RBC, red blood cell; SNOHb, *S*-nitrosohemoglobin; sGC, soluble guanylate cyclase.

REFERENCES

1. Alderton WK, Cooper CE, and Knowles RG. Nitric oxide synthases: structure, function and inhibition. *Biochem J* 357: 593–615, 2001.
2. Allen BW and Piantadosi CA. How do red blood cells cause hypoxic vasodilation? The SNO-hemoglobin paradigm. *Am J Physiol Heart Circ Physiol* 291: H1507–H1512, 2006.
3. Angelo M, Singel DJ, and Stamler JS. An S-nitrosothiol (SNO) synthase function of hemoglobin that utilizes nitrite as a substrate. *Proc Natl Acad Sci U S A* 103: 8366–8371, 2006.
4. Azarov I, Huang KT, Basu S, Gladwin MT, Hogg N, and Kim-Shapiro DB. Nitric oxide scavenging by red blood cells as a function of hematocrit and oxygenation. *J Biol Chem* 280: 39024–39032, 2005.
5. Buerk DG. Can we model nitric oxide biotransport? A survey of mathematical models for a simple diatomic molecule with surprisingly complex biological activities. *Annu Rev Biomed Eng* 3: 109–143, 2001.
6. Butler AR, Megson IL, and Wright PG. Diffusion of nitric oxide and scavenging by blood in the vasculature. *Biochim Biophys Acta* 1425: 168–176, 1998.
7. Chen K and Popel AS. Theoretical analysis of biochemical pathways of nitric oxide release from vascular endothelial cells. *Free Radic Biol Med* 41: 668–680, 2006.
8. Chen K and Popel AS. Vascular and perivascular NO release and transport: biochemical pathways of NOS1 and NOS3. *Free Radic Biol Med* 42: 811–822, 2007.
9. Condorelli P and George SC. In vivo control of soluble guanylate cyclase activation by nitric oxide: a kinetic analysis. *Biophys J* 80: 2110–2119, 2001.
10. El-Farra NH, Christofides PD, and Liao JC. Analysis of nitric oxide consumption by erythrocytes in blood vessels using a distributed multicellular model. *Ann Biomed Eng* 31: 294–309, 2003.
11. Giulivi C, Kato K, and Cooper CE. Nitric oxide regulation of mitochondrial oxygen consumption I: cellular physiology. *Am J Physiol Cell Physiol* 291: C1225–C1231, 2006.
12. Gladwin MT. Hemoglobin as a nitrite reductase regulating red cell-dependent hypoxic vasodilation. *Am J Respir Cell Mol Biol* 32: 363–366, 2005.
13. Gladwin MT, Lancaster JR Jr, Freeman BA, and Schechter AN. Nitric oxide's reactions with hemoglobin: a view through the SNO-storm. *Nat Med* 9: 496–500, 2003.
14. Gladwin MT, Wang X, Reiter CD, Yang BK, Vivas EX, Bonaventura C, and Schechter AN. S-Nitrosohemoglobin is unstable in the reductive erythrocyte environment and lacks O_2/NO-linked allosteric function. *J Biol Chem* 277: 27818–27828, 2002.
15. Gow AJ. Nitric oxide, hemoglobin, and hypoxic vasodilation. *Am J Respir Cell Mol Biol* 32: 479–482, 2005.
16. Guo X, Lu X, Ren H, Levin ER, and Kassab GS. Estrogen modulates the mechanical homeostasis of mouse arterial vessels through nitric oxide. *Am J Physiol Heart Circ Physiol* 290: H1788–H1797, 2006.
17. Haas TL and Duling BR. Morphology favors an endothelial cell pathway for longitudinal conduction within arterioles. *Microvasc Res* 53: 113–120, 1997.
18. Huang A, Sun D, Shesely EG, Levee EM, Koller A, and Kaley G. Neuronal NOS-dependent dilation to flow in coronary arteries of male eNOS-KO mice. *Am J Physiol Heart Circ Physiol* 282: H429–H436, 2002.
19. Hyduke DR and Liao JC. Analysis of nitric oxide donor effectiveness in resistance vessels. *Am J Physiol Heart Circ Physiol* 288: H2390–H2399, 2005.
20. Iwakiri Y, Satoh A, Chatterjee S, Toomre DK, Chalouni CM, Fulton D, Groszmann RJ, Shah VH, and Sessa WC. Nitric oxide synthase generates nitric oxide locally to regulate compartmentalized protein S-nitrosylation and protein trafficking. *Proc Natl Acad Sci U S A* 103: 19777–19782, 2006.
21. James PE, Lang D, Tufnell-Barret T, Milsom AB, and Frenneaux MP. Vasorelaxation by red blood cells and impairment in diabetes: reduced nitric oxide and oxygen delivery by glycated hemoglobin. *Circ Res* 94: 976–983, 2004.
22. Jeffers A, Xu X, Huang KT, Cho M, Hogg N, Patel RP, and Kim-Shapiro DB. Hemoglobin mediated nitrite activation of soluble guanylyl cyclase. *Comp Biochem Physiol A Mol Integr Physiol* 142: 130–135, 2005.
23. Jia L, Bonaventura C, Bonaventura J, and Stamler JS. S-nitrosohaemoglobin: a dynamic activity of blood involved in vascular control. *Nature* 380: 221–226, 1996.
24. Kashiwagi S, Kajimura M, Yoshimura Y, and Suematsu M. Nonendothelial source of nitric oxide in arterioles but not in venules: alternative source revealed in vivo by diaminofluorescein microfluorography. *Circ Res* 91: e55–e64, 2002.
25. Kavdia M. A computational model for free radicals transport in the microcirculation. *Antioxid Redox Signal* 8: 1103–1111, 2006.
26. Kavdia M and Popel AS. Venular endothelium-derived NO can affect paired arteriole: a computational model. *Am J Physiol Heart Circ Physiol* 290: H716–H723, 2006.
27. Kavdia M and Popel AS. Wall shear stress differentially affects NO level in arterioles for volume expanders and Hb-based O_2 carriers. *Microvasc Res* 66: 49–58, 2003.
28. Kleinbongard P, Schulz R, Rassaf T, Lauer T, Dejam A, Jax T, Kumara I, Gharini P, Kabanova S, Ozuyaman B, Schnurch HG, Godecke A, Weber AA, Robenek M, Robenek H, Bloch W, Rosen P, and Kelm M. Red blood cells express a functional endothelial nitric oxide synthase. *Blood* 107: 2943–2951, 2006.
29. Kollau A, Hofer A, Russwurm M, Koesling D, Keung WM, Schmidt K, Brunner F, and Mayer B. Contribution of aldehyde dehydrogenase to mitochondrial bioactivation of nitroglycerin: evidence for the activation of purified soluble guanylate cyclase through direct formation of nitric oxide. *Biochem J* 385: 769–777, 2005.
30. Lacza Z, Pankotai E, Csordas A, Gero D, Kiss L, Horvath EM, Kollai M, Busija DW, and Szabo C. Mitochondrial NO and reactive nitrogen species production: does mtNOS exist? *Nitric Oxide* 14: 162–168, 2006.
31. Lancaster JR Jr. Simulation of the diffusion and reaction of endogenously produced nitric oxide. *Proc Natl Acad Sci U S A* 91: 8137–8141, 1994.
32. Lipowsky HH, Usami S, Chien S, and Pittman RN. Hematocrit determination in small bore tubes by differential spectrophotometry. *Microvasc Res* 24: 42–55, 1982.
33. Macarthur PH, Shiva S, and Gladwin MT. Measurement of circulating nitrite and S-nitrosothiols by reductive chemiluminescence. *J Chromatogr B Analyt Technol Biomed Life Sci* 2007 (in press).

34. Nase GP, Tuttle J, and Bohlen HG. Reduced perivascular PO_2 increases nitric oxide release from endothelial cells. *Am J Physiol Heart Circ Physiol* 285: H507–H515, 2003.
35. Rassaf T, Bryan NS, Maloney RE, Specian V, Kelm M, Kalyanaraman B, Rodriguez J, and Feelisch M. NO adducts in mammalian red blood cells: too much or too little? *Nat Med* 9: 481—482; author reply 482–483, 2003.
36. Rifkind JM, Nagababu E, and Ramasamy S. Nitric oxide redox reactions and red cell biology. *Antioxid Redox Signal* 8: 1193–1203, 2006.
37. Rogers SC, Khalatbari A, Gapper PW, Frenneaux MP, and James PE. Detection of human red blood cell-bound nitric oxide. *J Biol Chem* 280: 26720–26728, 2005.
38. Roy B and Garthwaite J. Nitric oxide activation of guanylyl cyclase in cells revisited. *Proc Natl Acad Sci U S A* 103: 12185–12190, 2006.
39. Sharan M and Popel AS. A two-phase model for flow of blood in narrow tubes with increased effective viscosity near the wall. *Biorheology* 38: 415–428, 2001.
40. Singel DJ and Stamler JS. Chemical physiology of blood flow regulation by red blood cells: the role of nitric oxide and S-nitrosohemoglobin. *Annu Rev Physiol* 67: 99–145, 2005.
41. Sonveaux P, Kaz AM, Snyder SA, Richardson RA, Cardenas-Navia LI, Braun RD, Pawloski JR, Tozer GM, Bonaventura J, McMahon TJ, Stamler JS, and Dewhirst MW. Oxygen regulation of tumor perfusion by S-nitrosohemoglobin reveals a pressor activity of nitric oxide. *Circ Res* 96: 1119–1126, 2005.
42. Stone JR and Marletta MA. Spectral and kinetic studies on the activation of soluble guanylate cyclase by nitric oxide. *Biochemistry* 35: 1093–1099, 1996.
43. Suematsu M, Suganuma K, and Kashiwagi S. Mechanistic probing of gaseous signal transduction in microcirculation. *Antioxid Redox Signal* 5: 485–492, 2003.
44. Tarpey MM and Fridovich I. Methods of detection of vascular reactive species: nitric oxide, superoxide, hydrogen peroxide, and peroxynitrite. *Circ Res* 89: 224–236, 2001.
45. Thomas DD, Liu X, Kantrow SP, and Lancaster JR, Jr. The biological lifetime of nitric oxide: implications for the perivascular dynamics of NO and O_2. *Proc Natl Acad Sci U S A* 98: 355–360, 2001.
46. Tsai AG, Acero C, Nance PR, Cabrales P, Frangos JA, Buerk DG, and Intaglietta M. Elevated plasma viscosity in extreme hemodilution increases perivascular nitric oxide concentration and microvascular perfusion. *Am J Physiol Heart Circ Physiol* 288: H1730–H1739, 2005.
47. Tsai AG, Cabrales P, Manjula BN, Acharya SS, Winslow RM, and Intaglietta M. Dissociation of local nitric oxide concentration and vasoconstriction in the presence of cell-free hemoglobin oxygen carriers. *Blood* 108: 3603–3610, 2006.
48. Tsoukias NM and Popel AS. Erythrocyte consumption of nitric oxide in presence and absence of plasma-based hemoglobin. *Am J Physiol Heart Circ Physiol* 282: H2265–H2277, 2002.
49. Vaughn MW, Huang KT, Kuo L, and Liao JC. Erythrocyte consumption of nitric oxide: competition experiment and model analysis. *Nitric Oxide* 5: 18–31, 2001.
50. Vaughn MW, Kuo L, and Liao JC. Estimation of nitric oxide production and reaction rates in tissue by use of a mathematical model. *Am J Physiol* 274: H2163–H2176, 1998.
51. Vukosavljevic N, Jaron D, Barbee KA, and Buerk DG. Quantifying the L-arginine paradox in vivo. *Microvasc Res* 71: 48–54, 2006.
52. Wolzt M, MacAllister RJ, Davis D, Feelisch M, Moncada S, Vallance P, and Hobbs AJ. Biochemical characterization of S-nitrosohemoglobin: mechanisms underlying synthesis, no release, and biological activity. *J Biol Chem* 274: 28983–28990, 1999.
53. Zani BG and Bohlen HG. Transport of extracellular l-arginine via cationic amino acid transporter is required during in vivo endothelial nitric oxide production. *Am J Physiol Heart Circ Physiol* 289: H1381–H1390, 2005.

Address reprint requests to:
Kejing Chen, Ph.D.
613 Traylor Building, 720 Rutland Ave.
Department of Biomedical Engineering
Johns Hopkins University School of Medicine
Baltimore, MD 21205

E-mail: kchen21@jhu.edu

Date of first submission to ARS Central, January 30. 2007; date of final revised submission, March 12, 2007; date of acceptance, March 20, 2007.

This article has been cited by:

1. Kejing Chen, Roland N. Pittman, Aleksander S. Popel. 2009. Hemorrhagic shock and nitric oxide release from erythrocytic nitric oxide synthase: A quantitative analysis. *Microvascular Research* **78**:1, 107-118. [CrossRef]
2. Kejing Chen , Roland N. Pittman , Aleksander S. Popel . 2008. Nitric Oxide in the Vasculature: Where Does It Come From and Where Does It Go? A Quantitative Perspective. *Antioxidants & Redox Signaling* **10**:7, 1185-1198. [Abstract] [Full Text] [PDF] [PDF Plus]
3. Xiaoping Liu, Parthasarathy Srinivasan, Eric Collard, Paula Grajdeanu, Jay L. Zweier, Avner Friedman. 2008. Nitric Oxide Diffusion Rate is Reduced in the Aortic Wall#. *Biophysical Journal* **94**:5, 1880-1889. [CrossRef]
4. K CHEN, B PIKNOVA, R PITTMAN, A SCHECHTER, A POPEL. 2008. Nitric oxide from nitrite reduction by hemoglobin in the plasma and erythrocytes. *Nitric Oxide* **18**:1, 47-60. [CrossRef]